



This is a repository copy of *Multiple evolutionary pathways lead to vancomycin resistance in Clostridioides difficile*.

White Rose Research Online URL for this paper:

<https://eprints.whiterose.ac.uk/203433/>

Version: Submitted Version

Preprint:

Buddle, J.E. orcid.org/0000-0002-7259-0527, Wright, R.C.T. orcid.org/0000-0002-8095-8256, Turner, C.E. orcid.org/0000-0002-4458-9748 et al. (3 more authors) (Submitted: 2023) Multiple evolutionary pathways lead to vancomycin resistance in *Clostridioides difficile*. [Preprint - bioRxiv] (Submitted)

<https://doi.org/10.1101/2023.09.15.557922>

© 2023 The Author(s). This preprint is made available under the CC-BY-NC-ND licence (<https://creativecommons.org/licenses/by-nc-nd/4.0/>).

Reuse

This article is distributed under the terms of the Creative Commons Attribution-NonCommercial-NoDerivs (CC BY-NC-ND) licence. This licence only allows you to download this work and share it with others as long as you credit the authors, but you can't change the article in any way or use it commercially. More information and the full terms of the licence here: <https://creativecommons.org/licenses/>

Takedown

If you consider content in White Rose Research Online to be in breach of UK law, please notify us by emailing eprints@whiterose.ac.uk including the URL of the record and the reason for the withdrawal request.



eprints@whiterose.ac.uk
<https://eprints.whiterose.ac.uk/>

Multiple evolutionary pathways lead to vancomycin resistance in *Clostridioides difficile*

Jessica E. Buddle¹, Rosanna C. T. Wright², Claire E. Turner¹, Roy R. Chaudhuri¹, Michael A. Brockhurst^{2*}, Robert P. Fagan^{1*}

Affiliations:

¹Molecular Microbiology, School of Biosciences, University of Sheffield, Sheffield S10 2TN, UK

²Division of Evolution and Genomic Sciences, University of Manchester, Manchester M13 9PT, UK

*To whom correspondence should be addressed: r.fagan@sheffield.ac.uk,
michael.brockhurst@manchester.ac.uk

1 **Abstract**

2 *Clostridioides difficile* is an important human pathogen, for which there are very limited
3 treatment options, primarily the glycopeptide antibiotic vancomycin. In recent years
4 vancomycin resistance has emerged as a serious problem in several Gram positive pathogens,
5 but high level resistance has yet to be reported for *C. difficile*, although it is not known if this
6 is due to constraints upon resistance evolution in this species. Here we show that resistance
7 to vancomycin can evolve rapidly under ramping selection but is accompanied by severe
8 fitness costs and pleiotropic trade-offs, including sporulation defects that would be expected
9 to severely impact transmission. We identified two distinct pathways to resistance, both of
10 which are predicted to result in changes to the muropeptide terminal D-Ala-D-Ala that is the
11 primary target of vancomycin. One of these pathways involves a previously uncharacterised
12 D,D-carboxypeptidase, expression of which is controlled by a dedicated two-component
13 signal transduction system. Our findings suggest that while *C. difficile* is capable of evolving
14 high-level vancomycin resistance, this outcome may be limited clinically due to pleiotropic
15 effects on key pathogenicity trains. Moreover, our data provide a mutational roadmap to
16 inform genomic surveillance.

17 Introduction

18 *Clostridioides difficile* is the most common cause of antibiotic-associated diarrhoea
19 worldwide, resulting in significant morbidity and mortality¹ that places a huge burden on
20 healthcare systems^{2,3}. Most cases of nosocomial *C. difficile* infection (CDI) follow recent
21 antibiotic treatment, which, through altering microbial diversity in the colon, reduces
22 microbiota-mediated colonisation resistance⁴. Although restoring microbial community
23 diversity through faecal microbiota transplantation (FMT) is a potential future treatment for
24 CDI⁵, current treatment relies on additional antibiotics, most commonly metronidazole or
25 vancomycin. While these can resolve the CDI, they further exacerbate damage to the
26 microbiota, leading to recurrent CDI in up to 25% of cases⁶. Due to increasing incidence of
27 resistance and consequently poor patient outcomes, use of metronidazole has declined in
28 recent years, and vancomycin is now the recommended front line antibiotic in the UK⁷.

29 Vancomycin is a glycopeptide antibiotic that binds to the terminal D-Ala-D-Ala
30 residues on peptidoglycan muropeptide precursors, sterically blocking transglycosylation and
31 transpeptidation reactions⁸. Although relatively slow to emerge, resistance to vancomycin is
32 now found globally in *Staphylococcus aureus* (VRSA) and is widespread in several
33 *Enterococcus* spp. (VRE)^{9,10}. Vancomycin resistance in Enterococci is usually associated with
34 one of a number of *van* gene clusters which encode the enzymes that modify peptidoglycan
35 to remove the vancomycin binding site. Here, the D-Ala-D-Ala is replaced with either D-Ala-
36 D-Lac (e.g. *vanA*, also seen in VRSA), conferring high level resistance, or D-Ala-D-Ser (e.g.
37 *vanG*), conferring low level resistance¹¹. Vancomycin susceptibility of *C. difficile* is not routinely
38 tested in clinical laboratories making monitoring the emergence of resistance extremely
39 challenging. However, the effectiveness of vancomycin against CDI has declined over time¹²
40 and multiple case reports show reduced vancomycin susceptibility in individual clinical
41 isolates¹³. Although a complete *vanG* cluster is found in diverse *C. difficile* strains¹⁴, whether
42 this confers vancomycin resistance is unclear¹⁵. However, increased expression of the *vanG*
43 cluster does appear to be associated with reduced susceptibility to vancomycin. Moreover,
44 mutations in the *vanSR*-encoded two component system that reduce vancomycin
45 susceptibility through derepression of the *vanG* cluster, have been reported in both clinical
46 isolates and laboratory evolution experiments^{16,17}. Beyond such regulatory changes of the
47 *vanG* cluster, the molecular mechanisms underpinning the evolution of vancomycin
48 resistance in *C. difficile* remain unknown. For example, we do not know if other mutations

49 occurring within the *vanG* cluster or at other loci in the *C. difficile* genome contribute to
50 increasing resistance observed clinically. Moreover, whether the evolution of vancomycin
51 resistance is associated with pleiotropic phenotypic effects or fitness costs in *C. difficile* is
52 poorly understood.

53 To understand the evolutionary dynamics and molecular mechanisms of vancomycin
54 resistance in *C. difficile* we experimentally evolved ten replicate populations at increasing
55 concentrations of vancomycin. Within just 250 generations we observed the evolution of 16
56 to 32-fold increased vancomycin minimum inhibitory concentration (MIC). To identify the
57 causal genetic variants, we genome sequenced both endpoint resistant clones and whole
58 populations at multiple time-points during the evolution experiment, and reintroduced key
59 mutations, observed in the evolved resistant lineages, into the wild-type ancestral genetic
60 background. Evolution of increased vancomycin resistance was associated with mutations in
61 two distinct pathways, occurring either in *vanT* within the *vanG* cluster or in a gene encoding
62 a regulator of a previously uncharacterised D,D-carboxypeptidase. Mutations in either
63 pathway are predicted to modify the vancomycin target in the cell wall peptidoglycan and
64 both were associated with defects in growth and sporulation of varying severity. Together our
65 results propose a new mechanistic model for vancomycin resistance emergence in *C. difficile*,
66 potentially expanding the genetic determinants of resistance that should be monitored in
67 clinical genomic epidemiology. Moreover, our data suggest that the initial emergence of
68 vancomycin resistance in *C. difficile* in the clinic may be severely constrained by pleiotropic
69 fitness trade-offs with key transmission and virulence traits.

70 Results

71 Vancomycin resistance evolves rapidly in *C. difficile* during *in vitro* experimental evolution.

72 We first generated genetically barcoded ancestral strains in an avirulent background with
73 either wild-type or elevated mutation rates. Specifically, R20291, a clinically relevant ribotype
74 027 *C. difficile* strain, was rendered avirulent through complete deletion of 18 kb spanning
75 the entire PaLoc that includes the genes encoding both major toxins and associated
76 regulatory proteins, creating strain R20291 Δ PaLoc. A subsequent deletion, removing the
77 *mutSL* genes encoding a DNA-damage repair system, generated a hypermutable variant
78 R20291 Δ PaLoc Δ mutSL, with an approximately 20-fold higher mutation rate than the wild-
79 type. Five distinct derivatives of each ancestral strain were then generated through
80 introduction of a 9-nucleotide barcode sequence downstream of the *pyrE* gene, resulting in
81 10 individually barcoded replicate lines used in the evolution experiment (R20291 Δ PaLoc
82 *pyrE*::barcode 1-5; R20291 Δ PaLoc Δ mutSL *pyrE*::barcode 7-11). Each of the 10 barcoded
83 strains was used to inoculate a 6-well plate containing media supplemented with vancomycin
84 at 0.25x, 0.5x, 1x, 2x, 4x, and 8x the initial MIC of 1 μ g/ml. Populations were passaged every
85 48 h, whereby cells from the well with the highest antibiotic concentration permitting growth
86 were propagated in a 1:400 dilution to a fresh 6-well plate. This process was repeated for a
87 total of 30 serial transfers per replicate line, with adjustment of the vancomycin gradient over
88 time as the growth-permitting vancomycin concentration in each evolving line increased. Ten
89 corresponding control populations were propagated under equivalent conditions in the
90 absence of vancomycin. Populations underwent approximately 8.64 generations per transfer,
91 yielding approximately 259 generations throughout the course of the experiment.

92

93 Resistance evolved rapidly in all 10 replicate populations propagated with vancomycin
94 selection (Fig. 1a). Nine of the ten replicate lines evolved to grow in 2 μ g/mL vancomycin (an
95 apparent MIC of 4 μ g/mL, the EUCAST breakpoint) by the end of the second passage (P2) and
96 all ten grew in the presence of 8 μ g/mL (Bc2, 3, 4) or 16 (Bc1, 5, 7, 8, 9, 10, 11) μ g/mL
97 vancomycin by P30 (Fig. 1a). This was significantly accelerated in the hyper-mutable replicate
98 lines (Fig. 1b). At least six individual clones were isolated from each evolved population at
99 the end-point and their vancomycin MIC was determined. Of the 82 clones tested, 38 (46%)
100 had an MIC consistent with the vancomycin concentration permitting growth of the
101 population from which they were isolated, while the remainder had an MIC slightly lower

102 than expected [for 42 clones their MIC was 2-fold lower, whereas for 2 clones their MIC was
103 4-fold lower than the vancomycin concentration permitting growth of the population from
104 which they were isolated (Supplementary Data 1)], demonstrating that significant variation
105 existed within evolved populations by P30.

106

107 **Genetic bases of evolved vancomycin resistance**

108 To understand the genetic bases of increased vancomycin resistance in individual end-point
109 clones, one clone per replicate population that had an MIC representative of their population
110 was selected for whole genome sequencing. The parental strains for each barcoded lineage,
111 and one random endpoint clone from each replicate control population, were also
112 sequenced. For analyses we focused on mutations that were observed in the vancomycin
113 treated lines but never in ancestral or in control evolved clones because these are the most
114 likely to have evolved in response to vancomycin selection. Sequence variants unique to the
115 vancomycin-evolved clones were identified using Varscan¹⁸, validated with Breseq and IGV¹⁹
116 after mapping to the reference R20291 genome (Fig. 1b, Supplementary Data 2). We
117 observed between 1 and 3 unique mutations per genome in wild-type clones and between
118 14 and 26 in hypermutator clones from the vancomycin treatment. Within gene SNPs
119 accounted for 43% of the variants, of which 67.4% were nonsynonymous and 32.6% were
120 synonymous. Frameshifts accounted for a further 31% of identified unique mutations.

121

122 Parallel evolution, where mutations affecting the same locus arise in multiple independently
123 evolving replicate populations, is strong evidence for the action of selection and suggests a
124 potential role for these mutations in adaptation. In the 5 wild-type vancomycin selected lines
125 we observed parallel evolution occurring at three genomic loci: *vanT* in 3 clones, *CD3437* in 2
126 clones and *comR* in 2 clones. Whereas mutations in *vanT* and *CD3437* were mutually exclusive
127 in wild-type evolved clones, mutations in *comR* always co-occurred with mutations in *vanT*.
128 VanT is a putative Serine racemase (mutations in Bc3-5) encoded within a VanG-type cluster¹⁴
129 that was previously implicated in decreased vancomycin susceptibility in *C. difficile*¹⁶
130 (Supplementary Data 2). *CD3437* encodes a predicted two-component system histidine
131 kinase (mutations in Bc1 and 2), with its cognate response regulator encoded by *CD3438*.
132 These genes had not previously been implicated in vancomycin resistance, however the
133 nearby *CD3439* encodes a putative D,D-carboxypeptidase that likely plays a role in

134 modification of peptidoglycan through removal of the stem peptide terminal D-Ala. Based on
135 these predicted functions we propose renaming these genes *dacS* (*CD3437*, histidine kinase),
136 *dacR* (*CD3438*, response regulator) and *dacJ* (*CD3439*, D,D-carboxypeptidase). Consistent
137 with mutations at these loci playing key roles in vancomycin resistance, all five hypermutator
138 replicate lines had mutations in the *vanG* operon (1 had a nonsynonymous mutation in *vanT*
139 and 1 in *vanS*) or *dacS*, *dacR* (encoding the cognate response regulator) and *dacJ*.
140 Interestingly, one strain (Bc8) had mutations in both *dacS* and *CD1523* (*vanS*), encoding a two-
141 component system sensor histidine kinase that is thought to regulate the *vanG* operon in
142 response to vancomycin, suggesting that the two pathways to resistance are not entirely
143 mutually exclusive. *comR* encodes a homologue of the RNA degradosome component
144 PNPase, suggesting that RNA stability may play a role in the *vanT*-associated mechanism of
145 vancomycin resistance. Consistent with this possibility, in the third clone carrying a *vanT*
146 mutation we observed coexisting mutations affecting *maa*, encoding a putative maltose O-
147 acetyltransferase, and a 75 bp deletion that completely removed an intergenic region
148 downstream of *rpmH* and before *rnpA*, encoding another predicted component of the RNA
149 degradosome. By contrast, in the 2 clones carrying mutations in *dacS* we did not observe any
150 mutations likely to affect RNA stability: one clone had no additional unique mutations, while
151 the other had nonsynonymous mutations in *bclA3* and *CD3124*. *bclA3* encodes a spore surface
152 protein with no known function in vegetative cells, while *CD3124* encodes an orphan histidine
153 kinase of unknown function. Interestingly, four of the hypermutating lineages also had
154 mutations in *CD3124*, an identical frameshift mutation in all four.

155

156 **Vancomycin resistant clones display reduced fitness**

157 To assess the wider consequences of evolved vancomycin resistance for bacterial phenotype,
158 endpoint clones were phenotypically characterised for growth *in vitro*, sporulation efficiency
159 and cell morphology. All 10 strains displayed significantly impaired growth in rich liquid media
160 (Supplementary Fig. 1), with particularly severe defects apparent for Bc10 and 11. Several
161 strains were also impaired in sporulation (Supplementary Fig. 2), with a wide range of
162 phenotypes apparent, from a mild defect for Bc2 and 4 and delayed sporulation for Bc8, to
163 more severe defects for Bc7, Bc9 and 10 and complete loss of sporulation for Bc11. These
164 growth and sporulation defects were also accompanied by changes in cell length relative to
165 the parental wild type strain (Supplementary Fig. 3). Principal component analysis of the five

166 wild type-derived endpoint evolved clones (Fig. 1c) revealed all five resistant strains followed
167 similar evolutionary trajectories away from the parental wild type, associated with lower
168 sporulation efficiency and growth defects, albeit with divergence among replicate lines in the
169 extent of defects and cell size. However, there was no apparent sub-clustering by resistance
170 mechanism.

171

172 **Population dynamics in evolving populations**

173 Together the genome sequence data for end-point clones suggests that there are two
174 alternative mechanisms of vancomycin resistance, one involving *dacS* and the other involving
175 *vanT*. To better understand how selection acted upon these mechanisms we next performed
176 pooled population sequencing at passage 10, 20 and 30 to track mutation frequencies over
177 time (Fig. 2 and Supplementary Figs. 4 and 5). In total, discounting variants found in Bc1 P20,
178 we identified 535 unique variants across the 10 parallel populations and three timepoints.
179 We have removed Bc1 P20 from this analysis as the additional 520 variants identified in that
180 sample alone likely reflect random mutation due to the emergence of a spontaneous hyper-
181 mutator phenotype. Impacted genes clustered within 17 distinct functional classes by KEGG
182 analysis (Supplementary Fig. 6), with two component systems and ABC transporters being
183 particularly well-represented. Focusing on the two main routes to resistance identified in
184 endpoint clones, these data revealed highly contrasting selection dynamics, particularly in our
185 wild-type replicate populations: mutations in *dacS* rapidly rose to high frequency, reaching
186 fixation by P10. By contrast, mutations in *vanT* arose later and only reached fixation by P20
187 or 30, and were preceded by mutations at other sites which reached high frequency by P10
188 but that ultimately did not survive, being replaced by *vanT* mutants presumably conferring
189 higher levels of vancomycin resistance. The two preceding high frequency mutations in Bc3
190 (both T>TA) were very close together, separated by only 7 bp in an intergenic region
191 downstream of *CDO482*, encoding a uridine kinase, and approximately 250 bp upstream of
192 *glsA*, encoding a glutaminase. These mutations are outside of the likely promoter region²⁰ but
193 it is possible that they affect regulation of *glsA*. Interestingly, changes in glutamine
194 metabolism have previously been linked to vancomycin resistance in *Staphylococcus aureus*²¹.
195 The single high frequency mutation in Bc5 at P10 is a nonsynonymous substitution in *CD3034*,
196 introducing a Gly255Asp mutation in the encoded D-hydantoinase which may play a role in
197 the synthesis of D-amino acids. Taken together, these data suggest that *vanT* is not required

198 for first-step resistance; *vanT* mutations either provide higher-level vancomycin resistance,
199 allowing them to supplant earlier mutations, or they require potentiating mutations to arise
200 and be selected first. However, no consistent secondary mutations common to all populations
201 with *vanT* mutations were identified.

202

203 **Recapitulation of *dacS* mutations confirms role in resistance**

204 As the *dacJRS* cluster had not previously been implicated in vancomycin resistance, we
205 validated the role of DacS in vancomycin resistance by recapitulating individual mutations in
206 a clean genetic background. We chose the variant *dacS* alleles identified in Bc1 (714G>T), as
207 this is the sole unique mutation found in that strain, and the variant allele that evolved in
208 parallel in Bc8 and Bc9 (548T>C). Recapitulated strains carrying only the *dacS* mutation of
209 interest were constructed in the parental R20291 Δ *PaLoc* by allelic exchange. Introduction of
210 either mutation alone resulted in a 4-fold increase in the vancomycin MIC compared to the
211 parental strain, confirming that DacS is playing a significant role in the evolved resistance we
212 observed (Fig. 3a). AlphaFold prediction of the DacS structure yields a plausible dimer model
213 (Fig. 3b) that is highly similar to previously characterised histidine kinases²². The Bc1 and
214 Bc8/9 mutations described here both result in amino acid changes in the DacS cytoplasmic
215 domain: Bc1 Glu238Asp within the predicted catalytic ATPase (CA) domain and Bc8/9
216 Val183Ala within the dimerization and histidine phosphorylation (DHP) domain. The impact
217 of these mutations on the function of DacS is not clear but we hypothesised that DacS, along
218 with its cognate response regulator DacR, could be regulating the expression of the D,D-
219 carboxypeptidase encoded by *dacJ*. To examine this possibility, we extracted RNA from
220 R20291 Δ *PaLoc*, R20291 Δ *PaLoc* *dacSc*.714G>T and R20291 Δ *PaLoc* *dacSc*.548T>C, both in the
221 absence and presence of 0.5 μ g/ml vancomycin, and assessed the expression of *dacS*, *dacR*
222 and *dacJ* by qRT-PCR (Fig. 3c). Either point mutation resulted in a dramatic 4.8-94.6-fold
223 upregulation of expression of all three genes and this effect was independent of vancomycin.
224 It is highly likely, therefore, that the overexpression of DacJ and the resulting reduction in
225 vancomycin binding sites within the cell wall accounts for the reduction in vancomycin
226 susceptibility in both strains with mutated *dacS*. The genomic organisation in this region (Fig.
227 3d) and previous global transcription site mapping²⁰ suggests that *dacS* and *dacR* are
228 transcribed from a single promoter upstream of *dacR* and that *dacJ* is transcribed from its
229 own separate promoter. Our data demonstrate that both of these promoters are subject to

230 regulation by the DacS/DacR two component system, although it is not clear if the observed
231 effects are a result of constitutive activation of a TCS that positively regulates these promoters
232 or deactivation of a repressor (Fig. 3d).

233 Discussion

234 Vancomycin is one of the few antibiotics in routine use for treatment of CDI worldwide and is
235 now the frontline drug of choice in the UK⁷. High level vancomycin resistance is widespread
236 in *Enterococcus* spp. and in *S. aureus* but has yet to be reported in *C. difficile*, where there are
237 few verifiable reports of reduced susceptibility in clinical strains, despite anecdotal reports of
238 vancomycin treatment failure²⁶. However, it is not clear if this apparent lack of resistance
239 reflects an underlying constraint upon the emergence of resistance in this species or is simply
240 an artefact of a lack of routine monitoring in the clinic. Here we show using laboratory
241 experimental evolution that *C. difficile* can rapidly evolve high-level vancomycin resistance via
242 two alternative mechanisms, but that increased resistance is associated with severe
243 pleiotropic effects, including growth and sporulation defects, which may act to limit the
244 emergence of resistance in clinical settings.

245

246 Under ramping vancomycin selection, resistance emerged rapidly in all 10 replicate lines
247 reaching 16 to 32-fold higher MIC within approximately 250 generations. Whole genome
248 sequencing of individual clones from each population at the end of the evolution revealed
249 two evolutionary pathways to resistance, centring around mutations in *vanT*, encoding the
250 Serine/Alanine racemase component of a VanG-type cluster, and mutations in a cluster of
251 genes encoding a two component system and a D,D-carboxypeptidase (*dacJRS*). The VanG
252 cluster is common in *C. difficile* strains but its potential role in vancomycin resistance had
253 been disputed^{14,15}. More recently however, mutations in the VanRS two-component system
254 that derepress the rest of the cluster and reduce vancomycin susceptibility have been
255 identified in both laboratory evolution experiments and in clinical isolates^{16,17}. These
256 observations confirm that changes to the expression of genes in the VanG cluster can indeed
257 contribute to reduced vancomycin susceptibility. Interestingly we detected *vanS* mutations
258 only transiently in our evolution and none became fixed, suggesting they had only a limited
259 contribution to resistance or were accompanied by severe fitness defects (Fig. 4). In contrast,
260 mutations to *vanT* were common, fixing in four of ten replicate lines. Mutations in the *dacJRS*
261 cluster were also extremely commonly observed and often rose to high frequency, with
262 variant *dacS* alleles fixing in three populations (Bc1, 2 and 9), an identical *dacRc.532A>G*
263 variant fixing in two populations (Bc7 and 10) and a *dacJ* variant fixing in Bc9. Mutations in
264 *dacS* and *dacR* also transiently fixed in two further populations (Bc8 and 10 respectively) at

265 P20 before being subsequently outcompeted. Interestingly the *dacS* mutation identified in
266 Bc8 at P20 (548T>C) is identical to that observed in endpoint isolates from Bc9. None of these
267 genes had been previously linked to vancomycin resistance but the predicted D,D-
268 carboxypeptidase activity of DacJ points to a plausible mechanism through removal of the
269 terminal D-Ala residue in nascent peptidoglycan^{27,28} (Fig. 3d). We hypothesised that the two-
270 component system encoded by *dacS* and *dacR* was regulating expression of *dacJ*, providing a
271 mechanistic link for all of these mutations. This was confirmed by recapitulation of two
272 distinct *dacS* mutations (from Bc1 and Bc8/9) in a clean genetic background, leading to
273 derepression of both *dacJ* and the *dacSR* bicistronic operon. Importantly this effect was
274 independent of vancomycin, leaving open the possibility that the wild type system could still
275 contribute to vancomycin resistance in the appropriate permissive environmental condition.

276
277 Analysis of evolutionary dynamics over the course of the evolution also revealed intriguing
278 differences in the timing of *dacJRS* vs *vanT* mutations (summarised in Fig. 4). *dacJRS*
279 mutations had fixed by P10 in nearly every population in which they persisted to the end of
280 the evolution, the exception being Bc9 *dacJ* which first appeared and fixed at P20. However,
281 that population also had a superseding *dacS* mutation that had fixed by P10. By contrast,
282 mutations in *vanT* typically didn't fix until P20 or P30, although sometimes present at lower
283 frequency at earlier timepoints. Delayed emergence of *vanT* variants may also indicate a
284 reliance on preexisting potentiating mutations, although no consistent secondary mutations
285 were found in all *vanT* lineages. The two resistance mechanisms also seemed to be mutually
286 exclusive, *vanT* mutations did not co-occur with *dacJRS* in any population or endpoint isolate.
287 It is possible that early emergence of mutations in *dacJRS* precludes subsequent mutations to
288 *vanT* and commits the population to that pathway.

289
290 In all populations, emergence of resistance in our experiment was accompanied by severe, if
291 somewhat variable, fitness costs, importantly including severe sporulation defects in two
292 lineages. As the spore is the infectious form of *C. difficile* and an absolute requirement for
293 patient to patient transmission²⁹, these sporulation defects would likely have serious
294 consequences for the infectivity and onward transmission of evolved resistant isolates. The
295 genetic basis of the sporulation defects in these isolates is not clear, as sporulation is an
296 extremely complex and poorly understood cell differentiation process^{30,31}, but if a similar trait

297 were to emerge in a patient during vancomycin treatment this would be an evolutionary dead
298 end. These fitness defects may well explain delays to the emergence of vancomycin resistance
299 in the clinic. However, it is also possible that the accumulation of refining mutations would
300 eventually lead to gradually improving fitness as has been seen in long term evolution
301 experiments^{32,33}. Indeed, we saw extensive evidence of succession here, with early high
302 frequency mutations that conferred moderate increases in MIC being completely supplanted
303 by later variants, of presumably improved fitness. The potential for further evolution in our
304 experiment was also clear from the continual emergence of new variants, even at the final
305 timepoint. It remains to be seen how far towards full resistance *C. difficile* can go given the
306 enough time and the right conditions but, given the increasing reliance on vancomycin in the
307 treatment of CDI, it is crucial that we begin to understand the possible routes to resistance.
308 The question of how likely *C. difficile* vancomycin resistance is in the real world remains open
309 but this work, and other efforts towards understanding possible mechanisms of resistance,
310 will hopefully provide a roadmap to guide genomic surveillance efforts.

311 **Methods**

312 **Strains and Growth Conditions**

313 All strains used or generated in the course of this study are described in Supplementary Table
314 1. *C. difficile* was routinely cultured on brain heart infusion (BHI) agar and in tryptone yeast
315 (TY) broth. *C. difficile* was grown in an anaerobic cabinet (Don Whitley Scientific) at 37°C, with
316 an atmosphere composed of 80% N₂, 10% CO₂ and 10% H₂. Media was supplemented with
317 thiamphenicol (15 µg/mL) (Sigma) and colistin (50 µg/mL) (Sigma) as appropriate. For counter
318 selection against plasmids bearing the *codA* gene, *C. difficile* differential media with 5-
319 fluorocytosine (CDDM 5-FC) was used as described previously³⁴. *E. coli* was routinely cultured
320 in Luria-Bertani (LB) broth or agar at 37°C, and supplemented with chloramphenicol (15
321 µg/mL) (Acros Organics) or kanamycin (50 µg/mL) (Sigma) as appropriate.

322

323 **Molecular biology**

324 All oligonucleotides and plasmids are described in Supplementary Tables 2 and 3 respectively.
325 Plasmid miniprep, PCR purification and gel extractions were performed using GeneJET kits
326 (Thermo Fisher). High-fidelity PCR amplification was performed using Phusion polymerase
327 (NEB), and standard PCR amplification was performed using Taq mix red (PCRBIO), according
328 to manufacturers' instructions. Gibson assembly primers were designed using NEBBuilder
329 (NEB) and restriction digestion and DNA ligation was performed using enzymes supplied by
330 NEB. Plasmids were transformed into NEB5a (NEB) or CA434 competent *E. coli* cells according
331 to the NEB High Efficiency Transformation Protocol. The sequences of cloned fragments were
332 confirmed using Sanger sequencing (Genewiz, Azenta Life Sciences, Germany).

333

334 ***C. difficile* mutagenesis**

335 *C. difficile* strain R20291 was modified for use in evolution experiments and to recapitulate
336 individual mutations. Homology arms for introducing mutations onto the *C. difficile*
337 chromosome by allelic exchange were generated either by Gibson assembly of PCR products

338 or synthesised by Genewiz (Azenta Life Sciences) and then subsequently cloned between
339 BamHI and SacI sites in pJAK112²⁰, a derivative of pMTL-SC7215³⁴. Following confirmation by
340 Sanger sequencing, plasmids were transformed into *E. coli* CA434 and transferred to *C.*
341 *difficile* by conjugation³⁵. Homologous recombination was performed as previously
342 described³⁴ and mutations were confirmed by PCR and Sanger sequencing of mutated
343 regions.

344 R20291 was rendered avirulent via deletion of the complete pathogenicity locus (encoding
345 toxins A and B) using plasmid pJAK143³⁶, yielding strain R20291 Δ *PaLoc*. This strain was then
346 further modified by deletion of DNA repair operon *mutSL* to create a hyper-mutator strain.
347 1.2 kb up and downstream of the *mutSL* operon was amplified by PCR using oligonucleotides
348 RF2066 and RF2067, and RF2068 and RF2069 (Supplementary Table 2), respectively, and
349 cloned between BamHI and SacI sites in plasmid pJAK112. The resulting plasmid, pJEB002,
350 was then conjugated into R20291 Δ *PaLoc* and allelic exchange performed as described above,
351 yielding R20291 Δ *PaLoc* Δ *mutSL*. Enumeration of CFUs on BHI agar containing rifampicin (0.015
352 μ g/mL) suggested this strain has a mutation rate approximately 20-fold higher than
353 R20291 Δ *PaLoc*. Five barcoded variants of both R20291 Δ *PaLoc* and R20291 Δ *PaLoc* Δ *mutSL*
354 were then generated by insertion of unique sequencing barcodes. Briefly, pJAK081 (identical
355 to pJAK080²⁰ but in the pMTL-SC7215 backbone) was modified by introduction of a synthetic
356 DNA fragment containing a multiple cloning site and a 9 bp sequencing barcode (Barcode 1),
357 flanked by the *fdx* and *slpA* terminators, between the existing homology arms for insertion of
358 DNA between *CD0188* (*pyrE*) and *CD0189* in the R20291 genome. A second plasmid (pJAK202)
359 containing Barcode 2 was constructed in the same manner and the rest (pJAK203-205 and
360 207-211) were generated via site directed mutagenesis using pJAK201 as a template. These
361 ten plasmids were then used to generate R20291 Δ *PaLoc* Bc1-5 and R20291 Δ *PaLoc* Δ *mutSL*
362 Bc7-11. Recapitulated strains were generated by introducing point mutations into
363 R20291 Δ *PaLoc*. An approximately 2 kb synthetic DNA fragment, centred on the mutation of
364 interest, was cloned between BamHI and SacI sites in pJAK217, generating pJEB019
365 (*dacSc*.548T>C) and pJEB026 (*dacSc*.714G>T). The resulting plasmids were conjugated into
366 R20291 Δ *PaLoc*, and allelic exchange was performed as described above, generating
367 R20291 Δ *PaLoc* *dacSc*.548T>C and R20291 Δ *PaLoc* *dacSc*.714G>T respectively.

368

369 Evolution

370 Directed evolution of *C. difficile* was performed using a broth-based gradient approach in
371 which 10 individually barcoded parallel lines were evolved for a period of 30 passages. A 6-
372 well plate for each of the parallel lines was prepared for each passage using 4 mL of TY broth
373 with vancomycin, spanning a gradient of 0.25 to 8x the current MIC, as determined from the
374 most recent passage for each line, allowing the gradient to rise with increasing resistance.

375 The evolution was initiated using overnight cultures from single colonies, adjusted to OD_{600nm}
376 0.1. 10 µL was added to each well, before incubating for 48 h at 37°C. Plates were visually
377 inspected after 48 h and 10 µL of the well with the highest antibiotic concentration supporting
378 growth was used to inoculate the wells of the subsequent passage. For each parallel line, a
379 control well was passaged without antibiotic. 1 mL of a population, and the corresponding
380 control, was frozen at -80°C in 15% glycerol whenever the MIC increased; and after passages
381 10, 20 and 30.

382

383 gDNA Extraction

384 gDNA was obtained from *C. difficile* cultures using the phenol-chloroform method as
385 described previously³⁰. DNA concentration was quantified using Qubit, and purity was
386 assessed via microvolume spectrometry.

387

388 Sequencing

389 End-point (P30) isolates and respective controls were gained through plating P30 populations
390 and culturing single colonies. Vancomycin MICs were determined by agar dilution (described
391 below), and gDNA extraction and quantification were performed as above. Library prep
392 (Nextera XT Library Prep Kit (Illumina, San Diego, USA)) and 30x illumina sequencing (NovaSeq
393 6000, 250 bp paired end protocol) of isolates was performed at MicrobesNG (Birmingham,
394 UK). Reads were trimmed at MicrobesNG using Trimmomatic (v0.30)³⁷ with a sliding window
395 quality cut-off of Q15.

396 Pooled sequencing of the 10 evolved and 10 control populations was performed at 3
397 timepoints – P10, P20 and P30. 1 mL of the well with highest antibiotic concentration
398 supporting growth was taken after 48 h, harvested via centrifugation, and frozen at -20°C.
399 gDNA extraction and quantification were performed as above. Library prep (Nextera DNA Flex
400 Library Prep Kit (Illumina, San Diego, USA)) and 250x Illumina sequencing (NovaSeq 6000,
401 150bp paired end protocol) was performed at SNPsaurus (Oregon, USA). Reads were trimmed
402 using Trimmomatic (v0.39) with the following criteria: leading:3; trailing:3;
403 slidingwindow:4:15; minlen:36.

404

405 **Sequencing Analysis Pipeline: Isolates**

406 Trimmed reads were checked using FastQC (v0.11.9)³⁸ to ensure sufficient quality for analysis.
407 Analysis was primarily performed using a custom script, built based on a resistant mutant
408 analysis pipeline³⁹. Reads were aligned to the reference (*C. difficile* R20291, accession
409 number: FN545816) using BWA-mem (v0.7.17)⁴⁰ and sorted using SAMtools (v1.43)⁴¹.
410 Coverage across the genome was inferred using Bedtools (v2.30.0)⁴² genomcov and map
411 functions. PCR duplicates were removed via Picard (v2.25.2)
412 (<http://broadinstitute.github.io/picard/>). The mpileup utility within SAMtools (v1.43) was
413 used to generate the mpileup file required for Varscan. Variants were then called using
414 Varscan (v2.4.3-1)¹⁸ mpileup2cns (calling SNPs and indels) using the following parameters:
415 min-coverage 4; min-reads2 4; min-var-freq 0.80; p-value 0.05; variants 1; output-vcf 1. Here,
416 a minimum of 4 reads were required to support a variant, and the cut-off for variant calling
417 was 80%. Vcf files were annotated using snpEff (v5.0)⁴³. Variants were also called using Breseq
418 (v0.35.5)¹⁹, using default parameters, and putative variants were retained if detected in both
419 analysis pipelines. All variants were manually verified using IGV (v2.8.6)⁴⁴. Variants that were
420 also called in control lines were removed using Varscan (v2.4.3-1) compare, generating a list
421 of variants unique to vancomycin resistant lines.

422 Nonsynonymous mutations occurring within genes were plotted using a previously published
423 custom script in RStudio (v4.1.0) utilising the Plotrix package⁴⁵ to visualise parallel evolution.

424

425 Sequencing Analysis Pipeline: Populations

426 The 10 evolved and 10 control populations, sequenced at P10, P20 and P30, were evaluated
427 using a population analysis pipeline that followed the same custom script as for isolate
428 analysis, with modifications to SNP calling parameters and filtering. InSilicoSeq (v1.5.4)⁴⁶ was
429 used to rapidly simulate realistic sequencing data at a range of coverage depths (80x, 100x,
430 300x) based on the R20291 genome, with SNPs seeded at 5% frequency. Simulated sequences
431 were analysed using the custom pipeline, and a range of Varscan parameters (P-values, min-
432 coverage, min-reads2) were trialled to generate a set of parameters to accurately call variants
433 without false positives.

434 Varscan parameters used to call population variants were dependent on average coverage
435 depth, allowing a strong evidence base whilst calling low frequency variants. Samples were
436 separated by average coverage: the following Varscan (v2.4.3-1) mpileup2cns parameters
437 were used for samples with 100x or higher average coverage: min-coverage 80; min-var-freq
438 0.05; p-value 0.05; variants 1; output-vcf 1. A minimum of 4 reads were required to support
439 a variant, and the cut-off for variant calling was 5%. For samples with average coverage below
440 100x, the following Varscan (v2.4.3-1) mpileup2cns parameters were used: min-coverage 4;
441 min-reads2 4; min-var-freq 0.05; p-value 0.05; variants 1; output-vcf 1. As with high coverage
442 samples, a minimum of 4 reads were required to support a variant, meaning the minimum
443 variant frequency which could be called was inversely scaled ($4/\text{coverage at position}$), with a
444 minimum frequency of 5%. This process identified a list of variants within each line at each
445 time point, and their respective frequencies.

446 As in the isolate pipeline, population variants were filtered using Varscan (v2.4.3-1) compare,
447 removing variants that were also present in control lines to generate a list of variants unique
448 to vancomycin resistant lines. Further filtering of this dataset, again using Varscan (v2.4.3-1)
449 compare, discarded variants that never reached above 10% frequency by the end of the
450 evolution. Variants were also manually inspected to ensure no variants remained the same
451 frequency across all time points.

452 Mutations occurring within genes (except those in Bc1 P20) were coloured according to their
453 barcoded replicate line, and displayed in KEGG Mapper - Color⁴⁷ to view KEGG pathways.

454 Nonsynonymous mutations occurring within genes and rRNAs were plotted using a previously
455 published custom script in RStudio (v4.1.0) utilising the Plotrix package⁴⁵ to visualise
456 population dynamics, where point size indicated mutation frequency in the population.

457

458 **Strain fitness analysis**

459 Growth curves were performed anaerobically in 96 well plates using a Stratus microplate
460 reader (Cerillo). Overnight cultures of *C. difficile* were diluted to OD_{600nm} 0.05 and incubated
461 at 37°C for 1 h. Plate lids were treated with 0.05% Triton X-100 + 20% ethanol. Plates were
462 prepared using 200 µL of equilibrated culture. Samples were measured at minimum in
463 biological and technical triplicate. The OD_{600nm} was measured every 3 min over a 24 h period.
464 Data was plotted in Graph pad Prism (v9.0.2), and was analysed in RStudio (v4.1.0) using the
465 GrowthCurver package (v0.3.0)⁴⁸.

466 To assess sporulation efficiency, triplicate overnight *C. difficile* cultures were adjusted to
467 OD_{600nm} 0.01 and grown for 8 h. Cultures were then adjusted again to OD_{600nm} 0.01,
468 subcultured 1:100 into 10 mL BHIS broth, and grown overnight to obtain early stationary
469 phase spore-free cultures (T = 0). At T = 0, and the following 5 days, total viable counts were
470 enumerated by spotting 10-fold dilutions in technical triplicate onto BHIS agar with 0.1%
471 sodium taurocholate. Colonies were counted after 24 h incubation. Spore counts were
472 enumerated using the above method following heat treatment (65°C for 30 min).

473 To visualise cell morphology, *C. difficile* samples were harvested via centrifugation, washed
474 twice in PBS, and fixed in 4% paraformaldehyde; before harvesting and resuspension in dH₂O.
475 Samples were mounted in 80% glycerol, and imaged using a 100x Phase Contrast objective on
476 a Nikon Ti eclipse widefield imaging microscope using NIS elements software. Images were
477 analysed in Fiji (v2.9.0) using MicrobeJ (v5.131)⁴⁹.

478

479 **Vancomycin MICs**

480 MICs were obtained via standard agar dilution methods⁵⁰. Briefly, overnight cultures were
481 adjusted to OD_{600nm} 0.1. 2.5 µL of sample was spotted in biological triplicate and technical
482 duplicate onto BHI plates with ranging antibiotic concentrations. MICs were determined after
483 48 h incubation, and plates were imaged using a Scan 4000 colony counter (Interscience).

484

485 **Principal Component Analysis**

486 WT (Bc1-5) P30 resistant isolates were characterised in terms of their sporulation efficiency,
487 growth rate, MIC and cell length. These were compared, along with the WT ancestor from the
488 start of the evolution, in a principal component analysis (PCA). The PCA was computed using
489 the `prcomp()` function in Base R (<http://www.rproject.org/>), and visualised using the
490 `factoextra` package. The first 2 PC were plotted, as these accounted for 93% variance. The
491 loadings were added in their respective locations, and isolates were coloured based on
492 resistance mechanism.

493

494 **qRT-PCR**

495 Total RNA was extracted using the FastRNA pro blue kit (MP Biomedicals). Cells were grown
496 to an OD_{600nm} of approx. 0.4, and 2 volumes of RNA protect (Qiagen) were added. Cells were
497 incubated for a further 5 min, before harvesting via centrifugation. Cell pellets were stored at
498 -80°C. Pellets were resuspended in RNA Pro solution, and transferred to a tube containing
499 lysing matrix B (MP Biomedicals). Cells were lysed via FastPrep (2 cycles of 20 s, 6 m/s), and
500 centrifuged (16,200 x g, 4°C, 10 min) to remove insoluble cell debris. The supernatant was
501 transferred to a microfuge tube, and 300 µL chloroform (Sigma) was added. Samples were
502 centrifuged again (13,000 rpm, 4°C, 15 min), and the supernatant was precipitated at 20°C
503 overnight after addition of 500 µL 100% ethanol. After precipitation, RNA was harvested by
504 centrifugation (13,000 rpm, 4°C, 15 min), washed with 70% ethanol, and dried. Precipitated
505 RNA was resuspended in 50 µL nuclease-free water, residual DNA was removed using the
506 Turbo DNA-free kit (Invitrogen) and the RNA was cleaned and concentrated with the RNeasy
507 Minelute cleanup kit (Qiagen), as per manufacturers' instructions.

508 cDNA was generated using Superscript III (Invitrogen). 5 µg RNA was mixed with 2 µL dNTP
509 mix and 1 µL 100 mM random primer (Eurofins), heated at 65°C for 5 min, and cooled on ice.
510 8 µL 5X buffer, 2 µL 0.1M DTT (Invitrogen), 1 µL RiboLock RNase inhibitor (Thermo Scientific)
511 and 2 µL Superscript III were added, before incubation at 25°C (5 min), 50°C (30 min) and 70°C
512 (15 min). cDNA was adjusted to 40 ng/µL. RT negative controls were made as above, without
513 presence of Superscript III.

514 Expression was measured against an exact copy number control, via standardisation with a
515 plasmid containing one copy of each target DNA sequence⁵¹. *rpoA* was used as the
516 housekeeping gene to normalise results, and *rnpA* was used as an additional unrelated
517 control. A plasmid (pJEB029) was synthesised with the pUC-GW-Kan backbone (Genewiz),
518 containing approximately 200 bp target gene fragments of *dacS*, *dacR*, *dacJ*, *rpoA* and *rnpA*.
519 This was purified using the GeneJET plasmid miniprep kit (Thermo Fisher), and linearised using
520 NdeI (NEB) and diluted to known copy number (2×10^8 per µL). A qPCR mastermix was
521 assembled, containing 25 µL SYBR Green JumpStart Taq ReadyMix (Sigma), 7 µL MgCl₂ in
522 buffer (Sigma), forward and reverse primers (concentration determined by prior
523 optimisation) and nuclease-free water up to 45 µL. 5 µL of cDNA (40 ng/µL), 5 µL of RT
524 negative control, or 5 µL qPCR plasmid pJEB029 (diluted serially in lambda DNA (Promega))
525 were added, and qPCR was performed (BioRad CFX Connect Real Time System). Copy
526 numbers were calculated using BioRad CFX manager (v3.1), and data were analysed in
527 Microsoft Excel (2016) to generate copies per 1000 copies of *rpoA*. Data were graphed and
528 statistically analysed in Graph pad Prism (v9.0.2).

529

530 **Structural modelling of DacS**

531 DacS was modelled as a dimer using AlphaFold²³ and the resulting output files were visualised
532 using ChimeraX⁵².

533

534 **Statistics**

535 Statistical analysis was performed in Graphpad Prism (v9.0.2), and $P < 0.05$ was considered
536 significant. Data are presented as mean \pm SD, unless otherwise stated. Differences in growth
537 were analysed using the R package GrowthCurver outputs. A cross-correlation was performed
538 in RStudio using Hmisc and corrplot packages^{53,54}, which determined area under curve (AUC-
539 E) to be the most representative measure of growth. The differences in AUC-E, compared to
540 the control strain curves, were calculated using t-tests with Welch's correction. To test
541 differences in sporulation efficiency, AUC was chosen as a representative measure of
542 sporulation across all timepoints. AUC was calculated in Graphpad Prism (v9.0.2), and the
543 difference between AUC for P30 isolates was compared with the WT using a one-way ANOVA
544 with Brown-Forsythe and Welch's correction. Statistical analysis of cell length was performed
545 in Graphpad Prism (v9.0.2). Fiji (v2.9.0) MicrobeJ (v5.13l) cell length outputs for P30 isolates
546 were compared to the WT using a 1-way ANOVA with Brown-Forsythe and Welch's correction
547 to test for differences in cell length. To determine whether differences in expression of *dacS*,
548 *dacR*, *dacJ* and *rnpA* were significant between R20291 Δ *PaLoc*, R20291 Δ *PaLoc* *dacSc*.548T>C
549 and R20291 Δ *PaLoc* *dacSc*.714G>T, a two-way ANOVA with Dunnett's multiple comparisons
550 was performed in Graphpad Prism (v9.0.2).

551 **References**

- 552 1 Smits, W. K., Lyras, D., Lacy, D. B., Wilcox, M. H. & Kuijper, E. J. *Clostridium difficile*
553 infection. *Nat Rev Dis Primers* **2**, 16020 (2016). <https://doi.org/10.1038/nrdp.2016.20>
- 554 2 Aguado, J. M. *et al.* Highlighting clinical needs in *Clostridium difficile* infection: the
555 views of European healthcare professionals at the front line. *J Hosp Infect* **90**, 117-
556 125 (2015). <https://doi.org/10.1016/j.jhin.2015.03.001>
- 557 3 Lessa, F. C. *et al.* Burden of *Clostridium difficile* infection in the United States. *N Engl*
558 *J Med* **372**, 825-834 (2015). <https://doi.org/10.1056/NEJMoa1408913>
- 559 4 Lawley, T. D. *et al.* Antibiotic treatment of *Clostridium difficile* carrier mice triggers a
560 supershedder state, spore-mediated transmission, and severe disease in
561 immunocompromised hosts. *Infect Immun* **77**, 3661-3669 (2009).
562 <https://doi.org/10.1128/IAI.00558-09>
- 563 5 van Nood, E. *et al.* Duodenal infusion of donor feces for recurrent *Clostridium*
564 *difficile*. *N Engl J Med* **368**, 407-415 (2013). <https://doi.org/10.1056/NEJMoa1205037>
- 565 6 Louie, T. J. *et al.* Fidaxomicin versus vancomycin for *Clostridium difficile* infection. *N*
566 *Engl J Med* **364**, 422-431 (2011). <https://doi.org/10.1056/NEJMoa0910812>
- 567 7 Swart, N. *et al.* A cost-utility analysis of two *Clostridioides difficile* infection guideline
568 treatment pathways. *Clin Microbiol Infect* (2023).
569 <https://doi.org/10.1016/j.cmi.2023.06.018>
- 570 8 Rubinstein, E. & Keynan, Y. Vancomycin revisited - 60 years later. *Front Public Health*
571 **2**, 217 (2014). <https://doi.org/10.3389/fpubh.2014.00217>
- 572 9 Miller, W. R., Munita, J. M. & Arias, C. A. Mechanisms of antibiotic resistance in
573 enterococci. *Expert Rev Anti Infect Ther* **12**, 1221-1236 (2014).
574 <https://doi.org/10.1586/14787210.2014.956092>
- 575 10 McGuinness, W. A., Malachowa, N. & DeLeo, F. R. Vancomycin resistance in
576 *Staphylococcus aureus*. *Yale J Biol Med* **90**, 269-281 (2017).
- 577 11 Courvalin, P. Vancomycin resistance in gram-positive cocci. *Clin Infect Dis* **42 Suppl 1**,
578 S25-34 (2006). <https://doi.org/10.1086/491711>
- 579 12 Eubank, T. A., Gonzales-Luna, A. J., Hurdle, J. G. & Garey, K. W. Genetic mechanisms
580 of vancomycin resistance in *Clostridioides difficile*: a systematic review. *Antibiotics*
581 (*Basel*) **11** (2022). <https://doi.org/10.3390/antibiotics11020258>

- 582 13 Darkoh, C. *et al.* Emergence of clinical *Clostridioides difficile* isolates with decreased
583 susceptibility to vancomycin. *Clin Infect Dis* **74**, 120-126 (2022).
584 [https://doi.org:10.1093/cid/ciaa912](https://doi.org/10.1093/cid/ciaa912)
- 585 14 Peltier, J. *et al.* Genomic and expression analysis of the *vanG*-like gene cluster of
586 *Clostridium difficile*. *Microbiology (Reading)* **159**, 1510-1520 (2013).
587 [https://doi.org:10.1099/mic.0.065060-0](https://doi.org/10.1099/mic.0.065060-0)
- 588 15 Ammam, F. *et al.* The functional *vanGCd* cluster of *Clostridium difficile* does not
589 confer vancomycin resistance. *Mol Microbiol* **89**, 612-625 (2013).
590 [https://doi.org:10.1111/mmi.12299](https://doi.org/10.1111/mmi.12299)
- 591 16 Shen, W. J. *et al.* Constitutive expression of the cryptic *vanGCd* operon promotes
592 vancomycin resistance in *Clostridioides difficile* clinical isolates. *J Antimicrob*
593 *Chemother* **75**, 859-867 (2020). [https://doi.org:10.1093/jac/dkz513](https://doi.org/10.1093/jac/dkz513)
- 594 17 Wickramage, I. *et al.* The *vanR(Cd)* mutation 343A>G, resulting in a Thr115Ala
595 substitution, is associated with an elevated minimum inhibitory concentration (MIC)
596 of vancomycin in *Clostridioides difficile* clinical isolates from Florida. *Microbiol Spectr*
597 **11**, e0377722 (2023). [https://doi.org:10.1128/spectrum.03777-22](https://doi.org/10.1128/spectrum.03777-22)
- 598 18 Koboldt, D. C. *et al.* VarScan: variant detection in massively parallel sequencing of
599 individual and pooled samples. *Bioinformatics* **25**, 2283-2285 (2009).
600 [https://doi.org:10.1093/bioinformatics/btp373](https://doi.org/10.1093/bioinformatics/btp373)
- 601 19 Deatherage, D. E. & Barrick, J. E. Identification of mutations in laboratory-evolved
602 microbes from next-generation sequencing data using breseq. *Methods Mol Biol*
603 **1151**, 165-188 (2014). [https://doi.org:10.1007/978-1-4939-0554-6_12](https://doi.org/10.1007/978-1-4939-0554-6_12)
- 604 20 Fuchs, M. *et al.* An RNA-centric global view of *Clostridioides difficile* reveals broad
605 activity of Hfq in a clinically important gram-positive bacterium. *Proc Natl Acad Sci U*
606 *S A* **118** (2021). [https://doi.org:10.1073/pnas.2103579118](https://doi.org/10.1073/pnas.2103579118)
- 607 21 Cui, L., Murakami, H., Kuwahara-Arai, K., Hanaki, H. & Hiramatsu, K. Contribution of a
608 thickened cell wall and its glutamine nonamidated component to the vancomycin
609 resistance expressed by *Staphylococcus aureus* Mu50. *Antimicrob Agents Chemother*
610 **44**, 2276-2285 (2000). [https://doi.org:10.1128/AAC.44.9.2276-2285.2000](https://doi.org/10.1128/AAC.44.9.2276-2285.2000)
- 611 22 Jacob-Dubuisson, F., Mechaly, A., Betton, J. M. & Antoine, R. Structural insights into
612 the signalling mechanisms of two-component systems. *Nat Rev Microbiol* **16**, 585-
613 593 (2018). [https://doi.org:10.1038/s41579-018-0055-7](https://doi.org/10.1038/s41579-018-0055-7)

- 614 23 Jumper, J. *et al.* Highly accurate protein structure prediction with AlphaFold. *Nature*
615 **596**, 583-589 (2021). <https://doi.org/10.1038/s41586-021-03819-2>
- 616 24 Hallgren, J. *et al.* DeepTMHMM predicts alpha and beta transmembrane proteins
617 using deep neural networks. *bioRxiv*, 2022.2004.2008.487609 (2022).
618 <https://doi.org/10.1101/2022.04.08.487609>
- 619 25 Jones, P. *et al.* InterProScan 5: genome-scale protein function classification.
620 *Bioinformatics* **30**, 1236-1240 (2014). <https://doi.org/10.1093/bioinformatics/btu031>
- 621 26 Molleti, R. R., Bidell, M. R. & Tataru, A. W. Fidaxomicin-associated hypersensitivity
622 reactions: report of a morbilliform drug eruption. *J Pharm Pract* **36**, 993-997 (2023).
623 <https://doi.org/10.1177/08971900221078780>
- 624 27 Ghosh, A. S., Chowdhury, C. & Nelson, D. E. Physiological functions of D-alanine
625 carboxypeptidases in *Escherichia coli*. *Trends Microbiol* **16**, 309-317 (2008).
626 <https://doi.org/10.1016/j.tim.2008.04.006>
- 627 28 Meziane-Cherif, D., Stogios, P. J., Evdokimova, E., Savchenko, A. & Courvalin, P.
628 Structural basis for the evolution of vancomycin resistance D,D-peptidases. *Proc Natl*
629 *Acad Sci U S A* **111**, 5872-5877 (2014). <https://doi.org/10.1073/pnas.1402259111>
- 630 29 Deakin, L. J. *et al.* The *Clostridium difficile spo0A* gene is a persistence and
631 transmission factor. *Infect Immun* **80**, 2704-2711 (2012).
632 <https://doi.org/10.1128/IAI.00147-12>
- 633 30 Dembek, M. *et al.* High-throughput analysis of gene essentiality and sporulation in
634 *Clostridium difficile*. *mBio* **6**, e02383 (2015). <https://doi.org/10.1128/mBio.02383-14>
- 635 31 Shen, A. *Clostridioides difficile* spore formation and germination: new insights and
636 opportunities for intervention. *Annu Rev Microbiol* **74**, 545-566 (2020).
637 <https://doi.org/10.1146/annurev-micro-011320-011321>
- 638 32 Bottery, M. J., Wood, A. J. & Brockhurst, M. A. Temporal dynamics of bacteria-
639 plasmid coevolution under antibiotic selection. *ISME J* **13**, 559-562 (2019).
640 <https://doi.org/10.1038/s41396-018-0276-9>
- 641 33 Hull, R. C. *et al.* Antibiotics limit adaptation of drug-resistant *Staphylococcus aureus*
642 to hypoxia. *Antimicrob Agents Chemother* **66**, e0092622 (2022).
643 <https://doi.org/10.1128/aac.00926-22>
- 644 34 Cartman, S. T., Kelly, M. L., Heeg, D., Heap, J. T. & Minton, N. P. Precise manipulation
645 of the *Clostridium difficile* chromosome reveals a lack of association between the

- 646 *tcdC* genotype and toxin production. *Appl Environ Microbiol* **78**, 4683-4690 (2012).
647 <https://doi.org/10.1128/AEM.00249-12>
- 648 35 Kirk, J. A. & Fagan, R. P. Heat shock increases conjugation efficiency in *Clostridium*
649 *difficile*. *Anaerobe* **42**, 1-5 (2016). <https://doi.org/10.1016/j.anaerobe.2016.06.009>
- 650 36 Ormsby, M. J. *et al.* An intact S-layer is advantageous to *Clostridioides difficile* within
651 the host. *PLoS Pathog* **19**, e1011015 (2023).
652 <https://doi.org/10.1371/journal.ppat.1011015>
- 653 37 Bolger, A. M., Lohse, M. & Usadel, B. Trimmomatic: a flexible trimmer for Illumina
654 sequence data. *Bioinformatics* **30**, 2114-2120 (2014).
655 <https://doi.org/10.1093/bioinformatics/btu170>
- 656 38 Andrews, S. *FastQC: a quality control tool for high throughput sequence data.*,
657 <<http://www.bioinformatics.babraham.ac.uk/projects/fastqc>> (2010).
- 658 39 Wright, R. C. T., Friman, V. P., Smith, M. C. M. & Brockhurst, M. A. Resistance
659 evolution against phage combinations depends on the timing and order of exposure.
660 *mBio* **10** (2019). <https://doi.org/10.1128/mBio.01652-19>
- 661 40 Li, H. & Durbin, R. Fast and accurate short read alignment with Burrows-Wheeler
662 transform. *Bioinformatics* **25**, 1754-1760 (2009).
663 <https://doi.org/10.1093/bioinformatics/btp324>
- 664 41 Li, H. *et al.* The Sequence Alignment/Map format and SAMtools. *Bioinformatics* **25**,
665 2078-2079 (2009). <https://doi.org/10.1093/bioinformatics/btp352>
- 666 42 Quinlan, A. R. & Hall, I. M. BEDTools: a flexible suite of utilities for comparing
667 genomic features. *Bioinformatics* **26**, 841-842 (2010).
668 <https://doi.org/10.1093/bioinformatics/btq033>
- 669 43 Cingolani, P. *et al.* A program for annotating and predicting the effects of single
670 nucleotide polymorphisms, SnpEff: SNPs in the genome of *Drosophila melanogaster*
671 strain w1118; iso-2; iso-3. *Fly (Austin)* **6**, 80-92 (2012).
672 <https://doi.org/10.4161/fly.19695>
- 673 44 Robinson, J. T. *et al.* Integrative genomics viewer. *Nat Biotechnol* **29**, 24-26 (2011).
674 <https://doi.org/10.1038/nbt.1754>
- 675 45 Harrison, E., Guymer, D., Spiers, A. J., Paterson, S. & Brockhurst, M. A. Parallel
676 compensatory evolution stabilizes plasmids across the parasitism-mutualism

- 677 continuum. *Curr Biol* **25**, 2034-2039 (2015).
678 <https://doi.org/10.1016/j.cub.2015.06.024>
- 679 46 Gourle, H., Karlsson-Lindsjo, O., Hayer, J. & Bongcam-Rudloff, E. Simulating Illumina
680 metagenomic data with InSilicoSeq. *Bioinformatics* **35**, 521-522 (2019).
681 <https://doi.org/10.1093/bioinformatics/bty630>
- 682 47 Kanehisa, M., Sato, Y. & Kawashima, M. KEGG mapping tools for uncovering hidden
683 features in biological data. *Protein Sci* **31**, 47-53 (2022).
684 <https://doi.org/10.1002/pro.4172>
- 685 48 Sprouffske, K. & Wagner, A. Growthcurver: an R package for obtaining interpretable
686 metrics from microbial growth curves. *BMC Bioinformatics* **17**, 172 (2016).
687 <https://doi.org/10.1186/s12859-016-1016-7>
- 688 49 Ducret, A., Quardokus, E. M. & Brun, Y. V. MicrobeJ, a tool for high throughput
689 bacterial cell detection and quantitative analysis. *Nat Microbiol* **1**, 16077 (2016).
690 <https://doi.org/10.1038/nmicrobiol.2016.77>
- 691 50 Clinical and Laboratory Standards Institute. Methods for antimicrobial susceptibility
692 testing of anaerobic bacteria; approved standard. (Clinical and Laboratory Standards
693 Institute, Wayne, PA, 2012).
- 694 51 Turner, C. E., Kurupati, P., Jones, M. D., Edwards, R. J. & Sriskandan, S. Emerging role
695 of the interleukin-8 cleaving enzyme SpyCEP in clinical *Streptococcus pyogenes*
696 infection. *J Infect Dis* **200**, 555-563 (2009). <https://doi.org/10.1086/603541>
- 697 52 Pettersen, E. F. *et al.* UCSF ChimeraX: Structure visualization for researchers,
698 educators, and developers. *Protein Sci* **30**, 70-82 (2021).
699 <https://doi.org/10.1002/pro.3943>
- 700 53 Harrell Jr, F. Hmisc: Harrell Miscellaneous. R package version 5.1-0. (2023).
- 701 54 Wei, T. & Simko, V. R package 'corrplot': visualization of a correlation matrix.
702 (Version 0.92). (2021).
703
704

705 **Data Availability**

706 Genome sequence data for parental strains, P30 resistant isolates and respective controls, as
707 well as pooled population sequencing data for resistant populations and controls at P10, 20
708 and 30 is deposited with the European Nucleotide Archive (ENA). The accession numbers for
709 these may be viewed in Supplementary Table 4.

710

711 **Acknowledgements**

712 We thank the Wolfson Light Microscopy Facility at the University of Sheffield, for assistance
713 with phase-contrast microscopy and the Bioinformatics Core, for training. We would also like
714 to thank Joseph A Kirk for construction of barcoding and $\Delta PaLoc$ plasmids, and for the
715 R20291 $\Delta PaLoc$ strain. JEB is supported by a studentship from the MRC Discovery Medicine
716 North (DiMeN) Doctoral Training Partnership (MR/R015902/1). RCTW is supported by BBSRC
717 grant (BB/T014342/1) and MAB by a Wellcome Trust Collaborative Award (220243/Z/20/Z).
718 CET is a Royal Society & Wellcome Trust Sir Henry Dale Fellow (208765/Z/17/Z).

719

720 **Author contributions**

721 JEB carried out all experiments, collected and analysed data, revised the sequencing analysis
722 pipelines, wrote and revised the manuscript. RCTW provided guidance on sequencing
723 analysis. CET designed experiments, provided guidance and provided tools for qRT-PCR
724 experiments and analysis. RRC provided guidance on bioinformatics analysis, provided
725 bioinformatics scripts, and analysed KEGG data. MAB designed the study, interpreted
726 evolution data, supervised the study, and revised the manuscript. RPF designed the study,
727 analysed data, supervised the study, wrote and revised the manuscript.

728

729 **Competing interests**

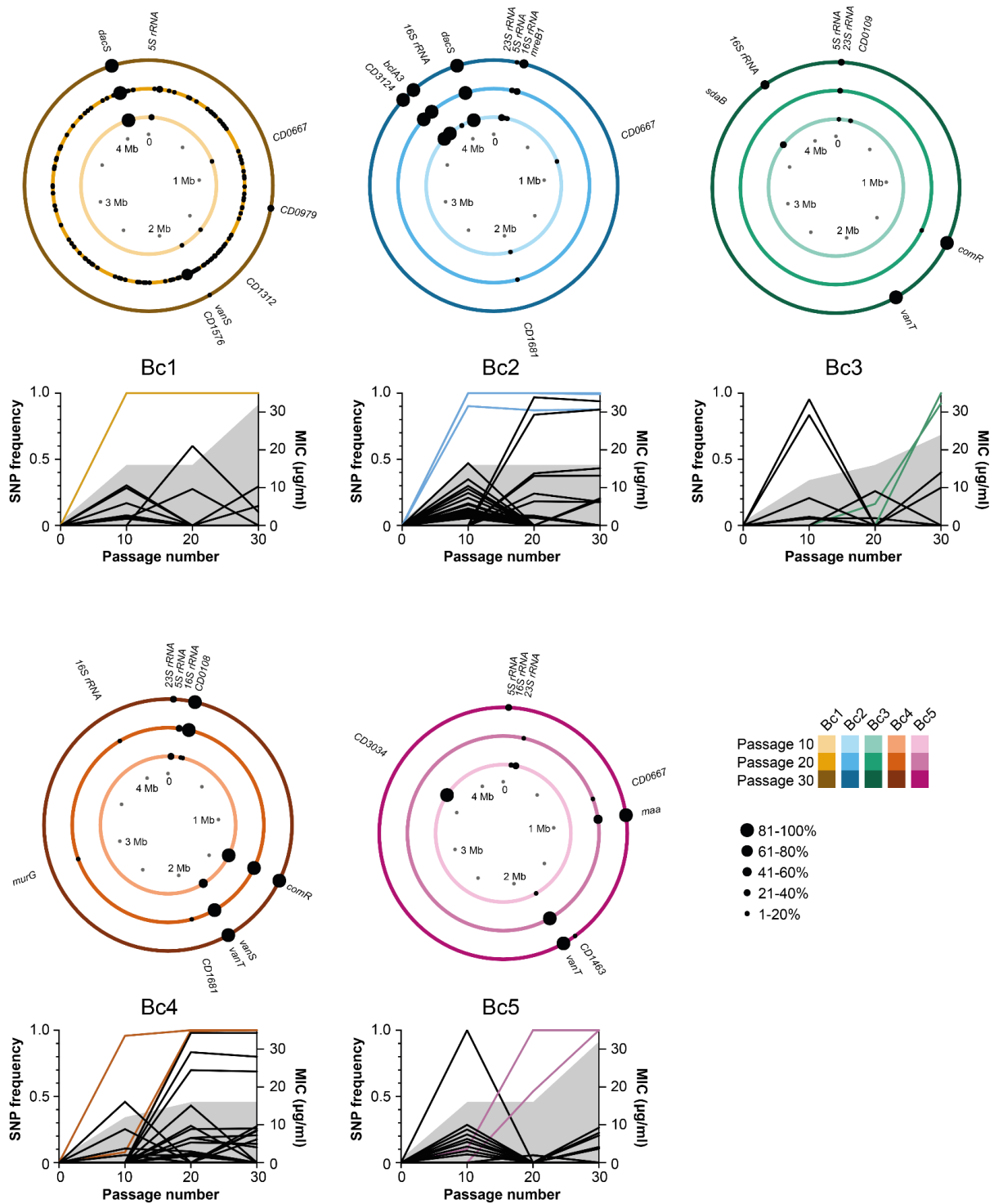
730 Summit Therapeutics Inc were industrial partners for JEB's MRC DiMeN iCASE PhD
731 studentship but had no input in study design, interpretation or manuscript preparation. The
732 authors declare no further competing interests.

733

734 **Materials and correspondence**

735 Requests should be addressed to Robert Fagan (email: r.fagan@sheffield.ac.uk) or Michael
736 Brockhurst (email: michael.brockhurst@manchester.ac.uk).

742 standard deviations of the apparent MIC for five wild type (open squares) and five hyper-
743 mutating (closed circles) populations. Linear regressions fitted to each data set, blue and pink
744 respectively, are significantly different by ANCOVA, $P=0.0008$. **c** Shown are the chromosomal
745 locations of non-synonymous variant alleles in isolated wild type (top) and hypermutating
746 (bottom) *C. difficile* end-point clones, excluding any mutations that were also identified in any
747 of the control strains. Each circle represents a single *C. difficile* genome, colour coded
748 according to population as indicated in the key on the left. A full list of all variants shown here
749 and including synonymous and intergenic mutations is included in Supplementary Data 2. **d**
750 Principal Component Analysis (PCA) of P30 isolates from populations Bc1-5 (coloured points)
751 vs the ancestral strain (black triangle), with PC1 versus PC2 plotted, accounting for 93%
752 variance. The loadings (sporulation efficiency, growth, MIC, cell length) are shown in
753 respective locations. Arrows show the evolutionary trajectories of wild-type replicate lines
754 from their ancestor in multivariate phenotype space.
755



756

757

758 **Fig. 2 Genomic location of gene variants over time.** Accumulation of variants in the wild type

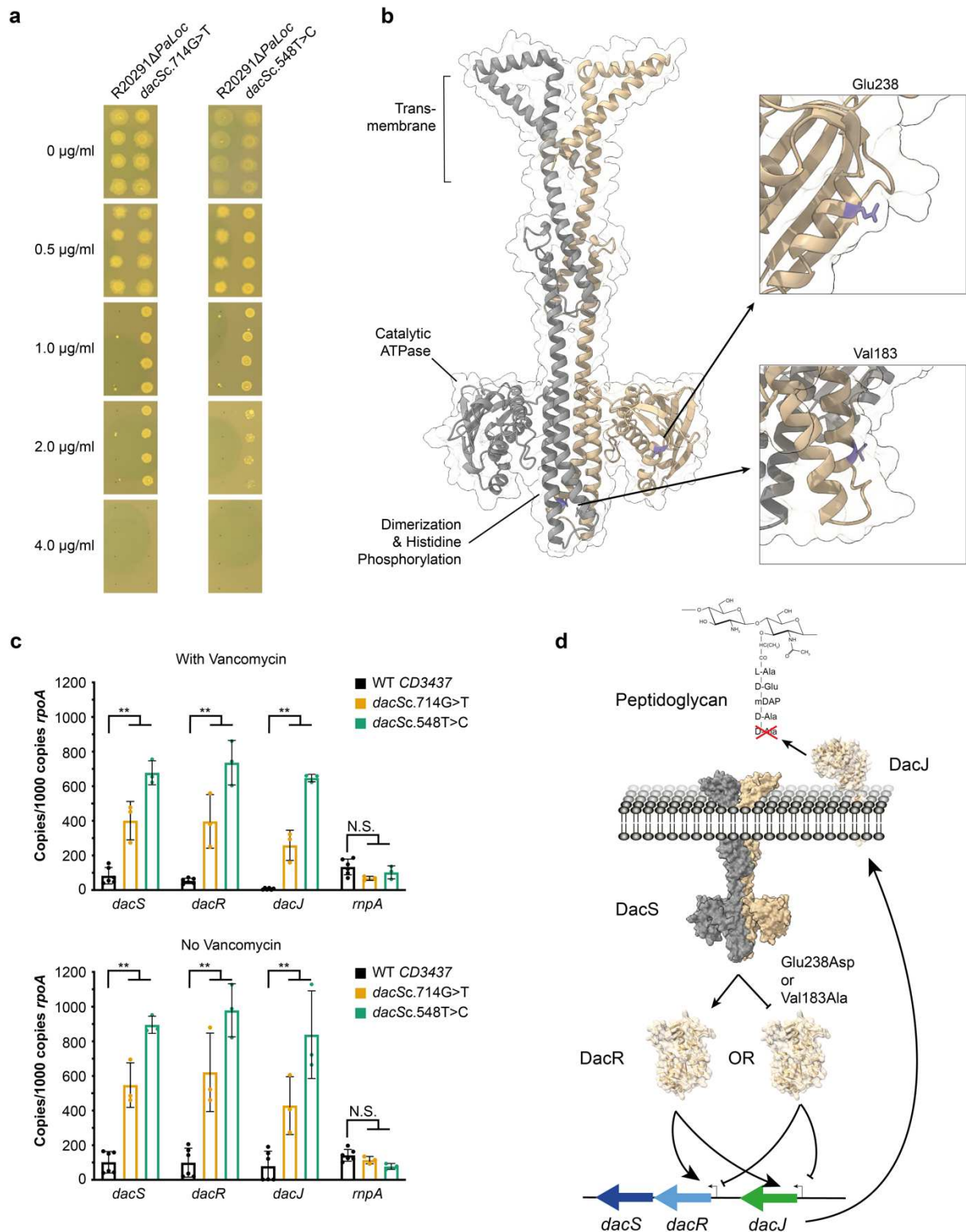
759 *C. difficile* lineages. Each circle plot represents the 4.2 Mb genome of a single evolving

760 population after 10 (inner ring), 20 (middle ring) and 30 passages (outer ring), with the

761 locations of non-synonymous within gene variants indicated with black circles and the

762 penetrance of each mutation in the population indicated by the size of the line

763 graphs show the frequency of all variants (intergenic, synonymous, non-synonymous,
764 frameshifts and nonsense) in each population. The vancomycin MIC for each population is
765 also indicated by the shaded region. Mutations also identified in the respective end point
766 clone (Fig. 1b) are highlighted by the coloured lines. Note population Bc1 evolved an apparent
767 hypermutator phenotype prior to P20, with 520 variants identified at that time point. For
768 simplicity only variants present in P10 and P30 are labelled. A full list of all variants shown
769 here, including those in Bc1 P20, is included in Supplementary Data 3.
770



771

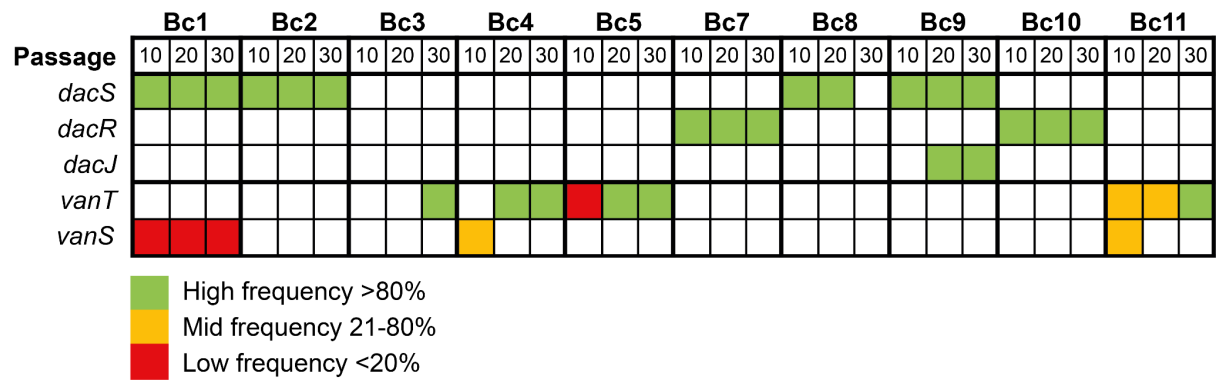
772

773 **Fig. 3 *dacS* mutations lead to dysregulation of *dacJRS*.** a Vancomycin MICs of R20291Δ*PaLoc*,

774 R20291Δ*PaLoc* *dacSc.714G>T* and R20291Δ*PaLoc* *dacSc.548T>C* as determined by agar

775 dilution. Assays were performed in biological triplicate and technical duplicate, four

776 representative spots are shown for each strain. **b** AlphaFold model of DacS as a dimer²³. The
777 transmembrane domains were identified using DeepTMHMM²⁴ and the Catalytic ATPase and
778 Dimerization and Histidine Phosphorylation domains were predicted using InterProScan²⁵.
779 The locations of Val183 and Glu238 are highlighted in purple on one chain. **c** qRT-PCR analysis
780 of *dacJRS* expression in R20291 Δ *PaLoc* (black bars), R20291 Δ *PaLoc* *dacSc.714G>T* (yellow
781 bars) and R20291 Δ *PaLoc* *dacSc.548T>C* (green bars). *rnpA*, which is implicated in the *vanT*
782 resistance pathway, was included as an additional unrelated control. Expression was
783 quantified against a standard curve and normalised relative to the house-keeping gene *rpoA*.
784 Assays were performed in biological and technical triplicate. Statistical significance was
785 calculated using a two-way ANOVA with Dunnett's multiple comparison, ** = $P < 0.001$. **d** Two
786 mechanisms by which DacS mutations could alter expression of *dacJRS*. Phosphorylated-DacR
787 could be an activator or repressor of the two promoters in the *dacJRS* locus, with DacS
788 Glu238Asp or Val183Ala substitutions either constitutively activating or inhibiting the
789 function of the TCS respectively. In either scenario, the consequence is over-expression of
790 DacJ which is then translocated to the cell surface where it can cleave the terminal D-Ala
791 residue in nascent peptidoglycan, thereby preventing vancomycin binding.



792

793

794 **Fig. 4 Two distinct pathways to resistance.** Relative frequencies and time of emergence of

795 mutations in genes *dacS*, *dacR*, *dacJ*, *vanT* and *vanS* across all ten evolving populations.